Journal of the Physical Society of Japan
Vol. 57, No. 9, September, 1988, pp. 3256-3261

Magneto-Optical Effects of the Wannier Exciton in a Biaxial ZnP_2 Crystal. I

Satoshi TAGUCHI, Takenari GOTO, Masayasu TAKEDA† and Giyuu KIDO†

Department of Physics, Faculty of Science, Tohoku University, Sendai 980
†Institute for Materials Research, Tohoku University, Sendai 980

(Received May 16, 1988)

An exciton absorption spectrum of a monoclinic ZnP_2 crystal for $E \parallel b$ polarization has been measured in magnetic fields up to 14 T. From behaviors of the exciton line series in the magnetic fields parallel to the *a*-, *b*- and *c*-axes, it is found that the exciton is of s-type and has a paramagnetic splitting with the *g*-factor of 4. Analyzing the diamagnetic shift in a biaxial crystal, we estimate exciton reduced masses and background dielectric constants in the *a*-, *b*- and *c*-axes to be $\mu_a=(0.39\pm0.03)m_0$, $\mu_b=(0.45\pm0.03)m_0$, $\mu_c=(0.15\pm0.01)m_0$, $\varepsilon_a=7.8\pm0.2$, $\varepsilon_b=10.0\pm0.2$ and $\varepsilon_c=9.7\pm0.2$, respectively.

§1. Introduction

A monoclinic ZnP_2 crystal gives us an absorption spectrum showing a very clear hydrogen-like series of a Wannier exciton.[1,2] Hence, this crystal is one of the most useful candidates for studying excitons. For $E \parallel c$ polarization, a direct allowed exciton series is observed near 800 nm in the reflectivity spectrum. For $E \parallel b$ polarization, the exciton transition is partially allowed so that the absorption coefficient is of the order of 10 cm^{-1}. Pevtsov *et al.*,[1] have found the exciton series up to $n=7$ in the absorption spectrum of the 1.2 mm thick crystal. The exciton binding energy scarcely depends on the crystal structure and locates between 42 and 48 meV.[3] These values are relatively large in spite of the small band gap energy of 1.6 eV. Despite that ZnP_2 has a stable Wannier type exciton, there has been no study concerning the magnetic properties of the free exciton as far as we know. The monoclinic form of ZnP_2 has a biaxial crystal structure. An example of the magneto-optical study of excitons in the biaxial crystal has been reported in InI by Ohno *et al.*[4] Analysis concerning the anisotropy, however, has not been made in their paper.

In this paper, a type of the exciton envelope function is determined from the magnetic field dependence of the exciton absorption spectrum for $E \parallel b$ polarization. Moreover, the anisotropic reduced mass of the exciton and the dielectric constant are estimated from the analysis of the diamagnetic shift.

§2. Experimental

Sample preparation is as follows. 6N pure zinc metal and 6N pure phosphorus were sealed in a silica ampule in vacuum. Reaction was taken place at 450°C in 24 hours, and then, black coloured flake crystals were grown in a two zone furnace in which the temperatures were kept at 1020°C and 450°C. The structure of the as-grown crystal was analyzed using a diffracto-meter and a X-ray Weissenberg camera. As a result, the crystal has a monoclinic structure with the space symmetry of C_{2h}^5 and the main surface contains *b*- and *c*-axes, as reported by Hegyi *et al.*[5] The platelet-like single crystal with the thickness of the order of 100 μ was immersed in pumped liquid helium and its absorption spectrum for $E \parallel b$ polarization in magnetic fields up to 4 T was measured by using a Jobin-Yvon U-1000 monochromator with the high resolution of 0.03 nm and using a small superconducting magnet.

For the measurements in high magnetic fields up to 14 T, the crystal was attached to

the sample holder of a liquid helium cryostat inside of a big resistive magnet.[6] A light beam from the halogen lamp was analyzed with a monochromator. Thus obtained monochromatic light went through an optical fiber and a linear polarizer until it reached the sample. The transmitted light was detected by a photomultiplier after passing through an optical fiber. The spectral resolution was 0.1 nm which was a little wronger than the former.

§3. Experimental Results and Discussion

3.1 Exciton absorption spectra in the magnetic field

Figure 1 shows the exciton absorption spectrum in $E//b$ polarization at 2 K. The $n=1$ line is asymmetric in shape and tails to the high energy side. This fact means that the $n=1$ level is lowest and the intraband scattering by phonons is dominant. A hydrogenic series of the exciton is clearly seen but the $n=3$, 4 lines are doublet, as obtained by Pevtsov *et al.*[1]

The exciton Rydberg constant and the series limit are estimated to be 47.1 meV and 1.6028 eV, respectively, from the energies of the $n=2$ line and the higher energy component of the $n=3$ doublet. In Table I are listed the observed peak energies of the exciton lines and the calculated ones from the above Rydberg constant and series limit. The measured energies of the higher energy components of $n=4$, 5 doublets are in good agreement with the calculated ones within the experimental errors, and hence a typical Wannier exciton

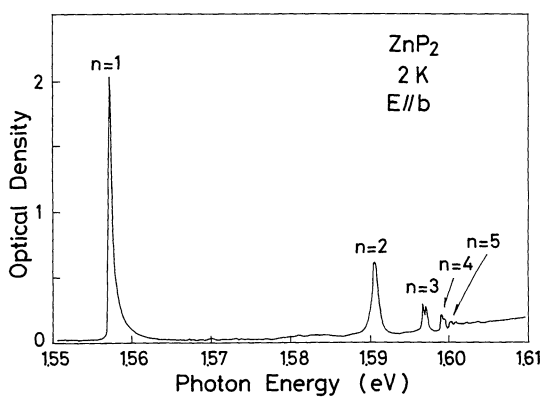

Fig. 1. Exciton absorption spectra of a monoclinic ZnP_2 crystal with the thickness of 0.2 mm in $E//b$ polarization without magnetic field at 2 K. An exciton hydrogenic series ($n=1$, 2, 3, 4, 5) is observed.

Table I. Experimental and calculated energies of the exciton absorption series.

Quantum number of excitons	Experimental energy (eV)	Calculated energy (eV)
$n=1$	1.5576	1.5557
$n=2$	1.5911	1.5911
$n=3$	1.5972 1.5976	1.5976
$n=4$	1.5995 1.5999	1.5999
$n=5$	1.6007 1.6010	1.6009

proves to exist in this crystal. Moreover, this coincidence suggests that the higher energy components of the $n=3$, 4, 5 lines are associated with the s-type exciton. The lower energy component of the $n=3$, 4, or 5 doublet, probably, originates from appearance of an exciton with a d-type envelope function due to the low crystal symmetry. For the $n=1$ line, however, the experimental energy is a little larger than the calculated one. This will be discussed in the next paper.

Figure 2 shows the absorption spectra in the $n\geqq 2$ exciton region for $E//b$ polarization in different magnetic fields perpendicular to the (100) surface. As the angle between the a- and c-axes is not 90° but 102.3°, the a-axis is nearly normal to the (100) surface, and hence, the magnetic field is slightly oblique to the a-axis. Hereafter, this orientation is represented by $H//a$. The $n=2$, 3 and 4 lines are denoted by open circles, open triangles and open squares, respectively. The lines denoted by closed symbols appear only in a finite magnetic field. Peak energies of marked lines are shown in Fig. 3 as a function of the magnetic field. Solid lines represent the theoretical curves[7] when the exciton energy obeys magnetic field dependence of the excitons with s-type envelope functions. Namely,

$$E_n(H)=E_n(0)+\sigma\frac{5n^4+n^2}{6}H^2, \quad n=2,3,4, \quad (1)$$

where H is the magnetic field, $E_n(0)$ the energy of the ns exciton at $H=0$, and σ the factor con-

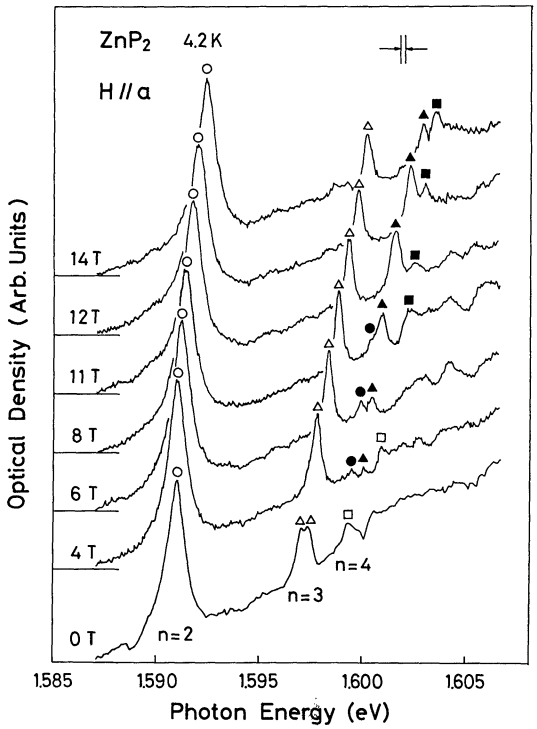

Fig. 2. Absorption spectra for the orientations $H//a$ in the different magnetic fields up to 14 T at 4.2 K. Open circles, open triangles and open squares show the $n=2$, 3 and 4 lines, respectively. Closed symbols denote new lines which appear only in the finite magnetic field.

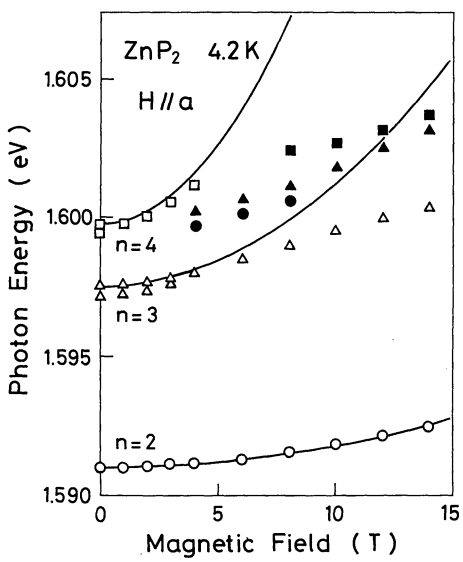

Fig. 3. Peak energies of exciton lines for orientation $H//a$ as a function of the magnetic field. Solid lines are theoretical curves of eq. (1) with an adjustable parameter $\sigma_a=5.4\times10^{-4}$ meV/T^2 deduced from the hydrogenic ns exciton model.

sisting of the dielectric constant and reduced mass. An adjustable parameter for $H//a$ configuration σ_a is determined as 5.4×10^{-4} meV/T^2. A good fit is obtained between the experimental points and the theoretical curves in all the measured magnetic fields for the $n=2$ line, in the fields below 6 T for the $n=3$ line and in the fields below 4 T for the $n=4$ line. In the view of such simple magnetic field dependence, the observed exciton lines are concluded to originate from an exciton with s-type envelope function. For the $n=3$ line, however, the theoretical curve deviates from the experimental points above 6 T and there appear three kinds of new lines denoted by closed symbols between the $n=3$ and $n=4$ lines. Such a deviation might be caused by the mixing with these new lines and/or by the fact that a low magnetic field approximation, $\gamma=\hbar\omega_c/2R_n\ll1$, is not valid in the higher magnetic fields. Here, ω_c is the cyclotron frequency and R_n the Rydberg constant of the ns exciton. The new lines may be associated with the excitons with the different envelope function from the s-type one.

For $H//c$, the absorption spectra in the $n\geqq1$ exciton region at different magnetic fields are shown in Fig. 4 and the exciton energies are plotted in Fig. 5 as a function of the magnetic field. In this configuration, all the lines split into a doublet in the magnetic field. Solid lines represent the following equation

$$E_n(H)=E_n(0)\pm\frac{1}{2}g\mu_BH+\sigma\frac{5n^4+n^2}{6}H^2,\quad n=1,2,3,4, \quad (2)$$

where H is the magnetic field in the c-direction, g the effective g-factor, and μ_B the Bohr magneton. Adjustable parameters for $H//c$, g_c and σ_c, are obtained as 4.0 and 2.1×10^{-4} meV/T^2, respectively. All the experimental points for the $n=1$, 2 lines agree well with the calculated curves except that a very weak line is observed at the center of the $n=1$ doublet. Open triangles and squares for the $n=3$, 4 lines, however, deviate from the theoretical curves above 11 T and 6 T, respectively, and the center energies of these doublets shift linearly with the magnetic field. Such deviation may be caused by violation of the weak

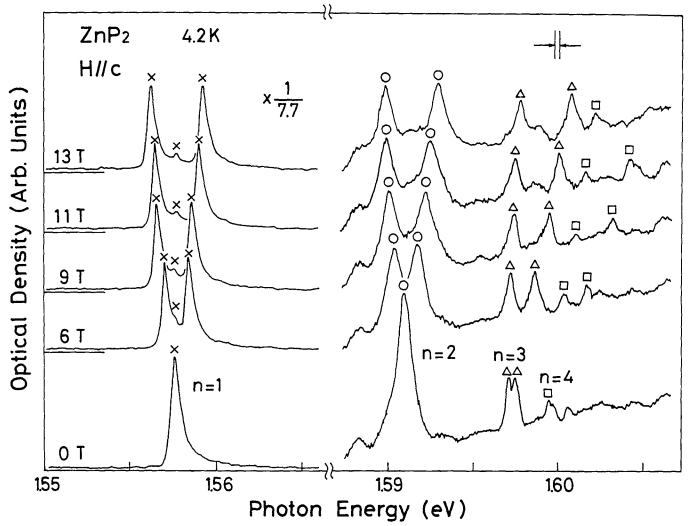

Fig. 4. Exciton spectra for orientation $H//c$ in the different magnetic fields at 4.2 K.

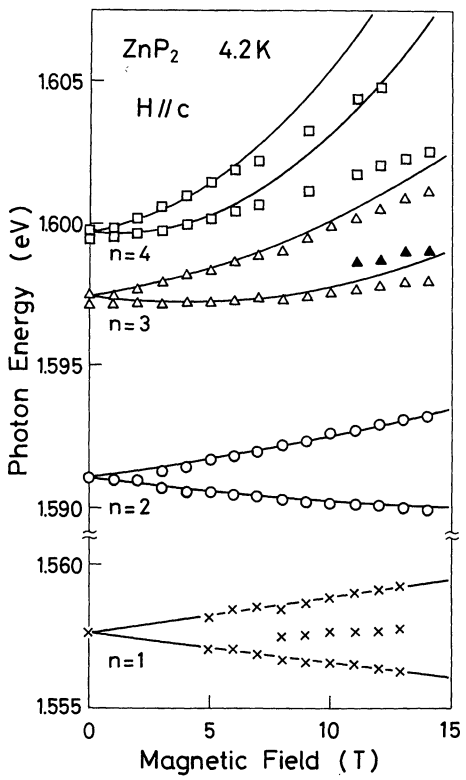

Fig. 5. Exciton energies vs the magnetic field for orientation $H//c$. Solid lines represent eq. (2) with adjustable parameters $g_c=4.0$ and $\sigma_c=2.1\times10^{-4}$ meV/T^2.

magnetic field approximation. In the magnetic fields less than a few tesla, a zero field splitting should be taken account.

For $H//b$, the absorption spectra in the different magnetic fields for $n\geqq2$ lines and the peak energies of the $n\geqq1$ lines as a function of the magnetic field are shown in Figs. 6 and 7, respectively. The calculated curves of eq. (2) with the adjustable parameters $g_b=4.1$ and $\sigma_b=6.3\times10^{-4}$ meV/T^2 are shown by solid lines in Fig. 7. In this configuration, the calculated curves give a good fit to the experimental points for the $n=1$, 2 lines. For the $n=3$ line, the calculated curves coincide with the experimental points below 5 T, but another Zeeman component appears below the calculated curves. Such complex structure seems to originate from appearance of the d-type exciton and its mixing with the s-type exciton, but the exact reason is not clear at present.

Origin of the paramagnetic splitting will be discussed in the next paper with respect to the magnetic field effect on the reflectivity spectrum for $E//c$ polarization corresponding to the direct allowed transition.

3.2 *Anisotropic exciton mass in the biaxial crystal*

In this section, the a-axis is assumed to be perpendicular to the c-axis and the a-, b- and

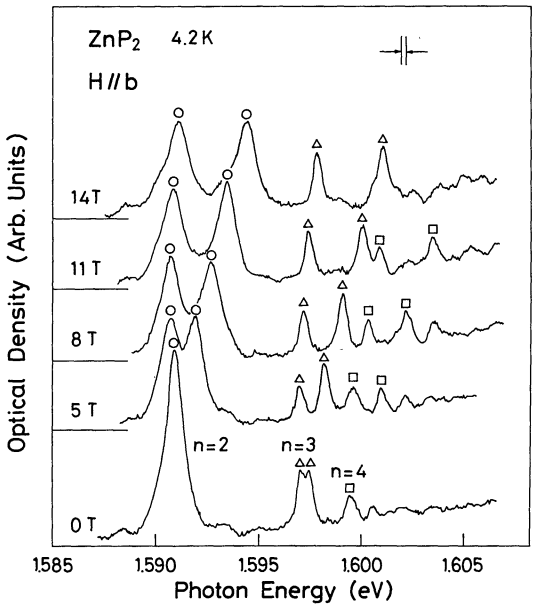

Fig. 6. Absorption spectra for $H//b$ in the different magnetic fields at 4.2 K.

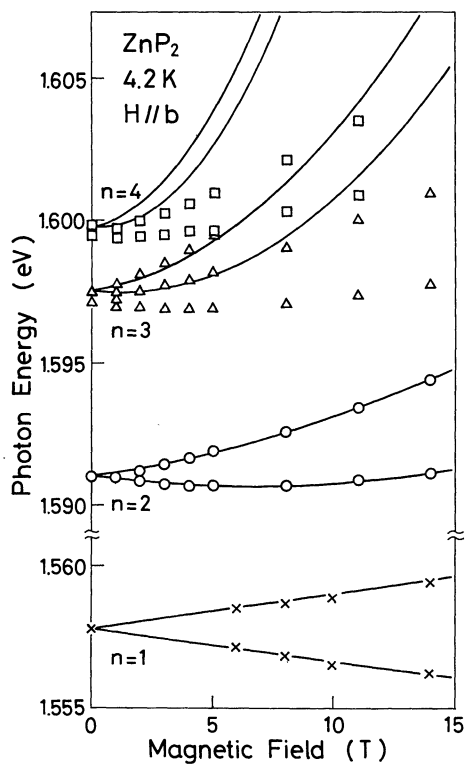

Fig. 7. Exciton energies vs the magnetic field for $H//b$. Solid lines show theoretical curves of eq. (2) with $g_b=4.1$ and $\sigma_b=6.3\times10^{-4}$ meV/T^2.

c-axes are assigned as x, z, and y axes, respectively. As the monoclinic ZnP_2 is a biaxial crystal, the reduced mass and the dielectric constant depend on the direction of the crystal axis. The x, y and z components of the reduced mass are denoted by μ_x, μ_y and μ_z, respectively, and the x, y and z components of the dielectric constant by ε_x, ε_y and ε_z, respectively. The Wannier exciton Hamiltonian without magnetic field is given by

$$\mathcal{H}=-\frac{\hbar^2}{2}\left(\frac{1}{\mu_x}\frac{\partial^2}{\partial x^2}+\frac{1}{\mu_y}\frac{\partial^2}{\partial y^2}+\frac{1}{\mu_z}\frac{\partial^2}{\partial z^2}\right)-\frac{e^2}{\sqrt{\varepsilon_y\varepsilon_z x^2+\varepsilon_z\varepsilon_x y^2+\varepsilon_x\varepsilon_y z^2}}. \tag{3}$$

If the coordinates x, y and z are changed into $\xi=\sqrt{(\mu_x/\mu)}x$, $\eta=\sqrt{(\mu_y/\mu)}y$, $\zeta=\sqrt{(\mu_z/\mu)}z$, respectively, eq. (3) can be rewritten as

$$\mathcal{H}=-\frac{\hbar^2}{2\mu}\left(\frac{\partial^2}{\partial\xi^2}+\frac{\partial^2}{\partial\eta^2}+\frac{\partial^2}{\partial\zeta^2}\right)-\frac{e^2}{\varepsilon}\frac{1}{\sqrt{\xi^2+\eta^2+\zeta^2}}+\frac{e^2}{\varepsilon}\left(\frac{1}{\sqrt{\xi^2+\eta^2+\zeta^2}}-\frac{1}{\sqrt{A\xi^2+B\eta^2+C\zeta^2}}\right). \tag{4}$$

Anisotropic parameters A, B, and C are given by

$$\left.\begin{aligned}A&=\frac{\mu}{\mu_x}\frac{\varepsilon_y\varepsilon_z}{\varepsilon^2},\\ B&=\frac{\mu}{\mu_y}\frac{\varepsilon_z\varepsilon_x}{\varepsilon^2},\\ C&=\frac{\mu}{\mu_z}\frac{\varepsilon_x\varepsilon_y}{\varepsilon^2},\end{aligned}\right\} \tag{5}$$

where μ is the average reduced mass, and ε the average dielectric constant. If μ and ε are defined as

$$\varepsilon=(\varepsilon_x\varepsilon_y\varepsilon_z)^{1/3}, \tag{6}$$

and

$$\frac{1}{\mu}=\frac{\varepsilon}{3}\left(\frac{1}{\varepsilon_x\mu_x}+\frac{1}{\varepsilon_y\mu_y}+\frac{1}{\varepsilon_z\mu_z}\right), \tag{7}$$

the following relation holds among A, B and C,

$$A+B+C=3. \tag{8}$$

The first and second terms in the right side of eq. (4) are the unperturbed Hamiltonian. The eigen value $E_n^{(0)}$ for the unperturbed Hamilto-

nian is given by

$$E_n^{(0)}=-\frac{e^4\mu}{2\hbar^2\varepsilon^2}\frac{1}{n^2}, \quad n=1, 2, 3, \cdots \tag{9}$$

The first order perturbation energy for 2 s Exciton $E_2^{(1)}$ is written as

$$E_2^{(1)}=E_2^{(0)}(f-1), \tag{10}$$

where

$$f=\frac{1}{2\pi}\int_0^{2\pi} d\phi \int_0^{\pi} \frac{\sin\theta\, d\theta}{\sqrt{(A\cos^2\phi+B\sin^2\phi)\sin^2\theta+C\cos^2\theta}}. \tag{11}$$

The diamagnetic terms of the exciton Hamiltonian in the magnetic fields H_x, H_y, and H_z are $(e^2/8c^2)(y^2/\mu_z+z^2/\mu_y)H_x^2$, $(e^2/8c^2)(z^2/\mu_x+x^2/\mu_z)H_y^2$, and $(e^2/8c^2)(x^2/\mu_y+y^2/\mu_x)H_z^2$, respectively. These terms give rise to the following diagonal elements for the 2 s exciton,

$$\left.\begin{aligned} 14\sigma_x H_x^2&=14\sigma\frac{\mu^2}{\mu_y\mu_z}H_x^2,\\ 14\sigma_y H_y^2&=14\sigma\frac{\mu^2}{\mu_z\mu_x}H_y^2,\\ 14\sigma_z H_z^2&=14\sigma\frac{\mu^2}{\mu_x\mu_y}H_z^2, \end{aligned}\right\} \tag{12}$$

where

$$\sigma=\frac{\hbar^4\varepsilon^2}{4c^2\mu^3e^2}. \tag{13}$$

On the other hand, the following relations are obtained from the reflectivity ratios among the x, y, z polarizations in transparant region:

$$\left.\begin{aligned} \varepsilon_x&=\left(\frac{0.09+1.91\sqrt{\varepsilon_y}}{1.91+0.09\sqrt{\varepsilon_y}}\right)^2,\\ \varepsilon_z&=\left(\frac{0.01+1.99\sqrt{\varepsilon_y}}{1.99+0.01\sqrt{\varepsilon_y}}\right)^2. \end{aligned}\right\} \tag{14}$$

Using the experimental values of σ_x, σ_y, σ_z, and eqs. (5)-(7), (12)-(14), anisotropic parameters, average dielectric constant ε and average reduced mass μ are represented as a function of ε_y. From eqs. (9)-(11) with the above values and the experimental value of the $n=2$ exciton energy, the dielectric constant ε_y is obtained as 9.7 ± 0.2. Thus, the exciton reduced masses and dielectric constants are estimated from eqs. (12)-(14) to be

$$\begin{aligned} \mu_x&=(0.39\pm0.03)m_0,\\ \mu_y&=(0.15\pm0.01)m_0,\\ \mu_z&=(0.45\pm0.03)m_0,\\ \varepsilon_x&=7.8\pm0.2,\\ \varepsilon_z&=10.0\pm0.2, \end{aligned}$$

where m_0 is a free electron mass. The obtained values of the dielectric constants are close to the static dielectric constant used in ref. 8.

Acknowledgements

The authors would like to thank Professor Y. Toyozawa of Chuo University, Dr. Y. Kayanuma of Tohoku University and Professor T. Komatsu of Osaka City University for fruitful discussions.

References

1) A. B. Pevtsov, S. A. Permogorov, A. V. Sel'kin, N. N. Syrbu and A. G. Umanets: Fiz. Tekh. Poluprovodn. **16** (1982) 1399. translation: Sov. Phys.-Semicond. **16** (1982) 897.
2) V. V. Sobolev and A. I. Kozlov: Phys. Status Solidi b **126** (1984) K59.
3) N. N. Syrbu and V. M. Mamaev: Fiz. Tekh. Poluprovodn. **17** (1983) 694. translation: Sov. Phys.-Semicond. **17** (1983) 433.
4) N. Ohno, M. Yoshida, K. Nakamura, J. Nakahara and K. Kobayashi: J. Phys. Soc. Jpn. **53** (1984) 1548.
5) I. J. Hegyi, E. E. Loebner, E. W. Poor Jr. and J. G. White: J. Phys. Chem. Solids **24** (1963) 333.
6) G. Kido and Y. Nakagawa: J. Magn. Soc. Jpn. **11** (1987) Suppl. p. 149.
7) J. H. Van Vleck: *The Theory of Electric and Magnetic Susceptibilities* (Oxford University Press, New York, 1932) p. 178.
8) A. V. Sel'kin, I. G. Stamov, N. N. Syrbu and A. G. Umanets: Pis'ma Zh. Eksp. Teor. Fiz. **35** (1982) 51. translation: Sov. Phys.-JETP Lett. **35** (1982) 57.